Alternative end-joining of DNA breaks

Schendel, Robin van

3

POLYMERASE THETA-MEDIATED END JOINING OF REPLICATION-ASSOCIATED DNA BREAKS IN *C. ELEGANS*

Sophie Roerink*, Robin van Schendel* and Marcel Tijsterman

*Co-first authors

Department of Toxicogenetics, Leiden University Medical Center, The Netherlands

Published in Genome Research 2014 March: 2014. 24: 954-962

ABSTRACT

DNA lesions that block replication fork progression are drivers of cancer-associated genome alterations, but the error-prone DNA repair mechanisms acting on collapsed replication are incompletely understood, and their contribution to genome evolution largely unexplored. Here, by whole genome sequencing of animal populations that were clonally propagated for over 50 generations, we identify a distinct class of deletions that spontaneously accumulate in *C. elegans* strains lacking translesion synthesis (TLS) polymerases. Emerging DNA double-strand breaks are repaired via an error-prone mechanism in which the outermost nucleotide of one end serves to prime DNA synthesis on the other end. This pathway critically depends on the A-family polymerase theta, which protects the genome against gross chromosomal rearrangements. By comparing the genomes of isolates of *C. elegans* from different geographical regions, we found that in fact most spontaneously evolving structural variations match the signature of polymerase Theta-Mediated End Joining (TMEJ), arguing that this pathway is an important source of genetic diversification.

INTRODUCTION

Identifying the mechanisms that fuel genome change is crucial for understanding evolution and carcinogenesis. Spontaneous mutagenesis is caused predominantly by misinsertions or slippage events of replicative polymerases that are missed by their proofreading domains, and not corrected by mismatch repair (Lynch 2008). Less frequently, but with a potentially much more detrimental effect, mutations can arise when DNA damage obstructs progression of DNA replication; and stalled replication forks eventually collapse, resulting in highly mutagenic double stranded breaks (DSBs). While error-free homologous repair, where the sister chromatid is used as a template, restores the original sequence, infrequent but highly mutagenic error-prone end joining processes can give rise to spontaneous deletions and tumor-promoting translocations (Mitelman et al. 2007).

To circumvent fork collapse at DNA damage, cells employ various alternative polymerases that are capable of incorporating nucleotides across DNA lesions, and are hence called translesion synthesis (TLS) polymerases. TLS acts on a wide variety of DNA lesions that can result from endogenous as well as exogenous genotoxic sources: DNA lesions that result from UV-light exposure, for instance, are efficiently bypassed by the well-conserved TLS polymerase eta (pol eta), inactivation of which in humans leads to the variant form of the skin cancer predisposition syndrome Xeroderma Pigmentosum (Johnson et al. 2007; Masutani et al. 1999b). Abundant *in vitro* studies demonstrate the involvement of TLS polymerases pol eta and pol kappa in bypass of lesions that are produced by endogenous reactive compounds, arguing that these polymerases are also essential for protection of the genome under unchallenged conditions (Fischhaber et al. 2002; Kusumoto et al. 2002; Haracska et al. 2000).

Although error-prone while replicating, and thus potentially causing misinsertions, TLS polymerases are thought to protect cells against the more mutagenic effects of replication fork collapse (Knobel and Marti 2011). Here, we investigate the contribution of TLS polymerases on the maintentance of genome stability and the mechanisms acting on stalled DNA replication, by characterizing *C. elegans* strains that are defective for the Y-family polymerases pol eta and pol kappa. Unexpectedly, we found that DSBs resulting from replication blocking endogenous lesions are not repaired via canonical DSB repair pathways but through an error-prone repair mechanism that critically depend on the A-family DNA polymerase theta (pol theta).

RESULTS

TLS polymerases protect genomes against spontaneous deletions

In previous work, we established the role of the *C. elegans* homologs of TLS polymerases pol eta (POLH-1) and pol kappa (POLK-1) in protection against a wide range of exogenous DNA damaging agents (Roerink et al. 2012). In these studies, we also sporadically observed readily recognizable mutant phenotypes during normal culturing of *polh-1polk-1* double mutant animals, which prompted us to suspect a prominent role for these Y-family of TLS polymerases in the prevention of spontaneous mutations (Figure S1). To address the nature of this increased mutagenesis in an unbiased way, we cultured populations of animals with specific defects in TLS for 60 generations, thus allowing spontaneous mutations to accumulate, and then sequenced their genomes (Figure 1A, Table S1 and Supplemental data file). Mutation accumulation (MA) lines of a wild-type strain (Bristol N2) and of the mismatch repair deficient strain *msh-6* - for which an ~100-fold higher mutation frequency has been reported (Tijsterman et al. 2002) - were sequenced as references. All

genomes have been sequenced with a minimal 12 fold base coverage (Table S1).

Although pol eta and pol kappa have reduced accuracy while replicating from undamaged as well as damaged DNA templates (Matsuda et al. 2000; Ohashi et al. 2000), we found that these proteins hardly contribute to base substitution processes or microsatellite instability under normal growth conditions: no significant elevation in the substitution or microsatellite mutation rates were found in *polh-1polk-1* worms as compared to wild-type controls (Figure 1B), which argues that another class of genetic changes must be responsible for the observed mutator phenotype. To detect other structural variations, we employed Pindel software, developed to identify deletions and/or insertions in whole-genome sequencing data (Ye et al. 2009). Strikingly, a unique class of deletions emerged in *polh-1* and *polh-1polk-1* mutants, which were not associated with repetitive loci, with sequences able to adopt stable secondary structure (*e.g.* G4 DNA), or with any other obvious genomic trait, and occurred at seemingly random locations throughout the genome (Figures 1C and S2). The vast majority of deletions ranged between 50 and 200 bp in size, with just a few exceptions being larger or smaller (Figure 1D). The median size, of 107 bp, was similar for deletions derived from either *polh-1* or *polh-1polk-1*-mutant animals (Figure 1D). Control wild-type and *msh-6* samples did not display any mutations from this class. Deletions occurred in *polh-1* single mutants with a rate of ~0.4 per animal generation, which translates to an average of ~0.03 deletion per genome per cell division. *polk-1* single mutants hardly suffered from deletions; however, *polh-1polk-1* double mutants had 5-fold increased rates of deletion induction as compared to *polh-1* single mutant animals, implying that *C. elegans* pol eta and pol kappa function redundantly on a subset of endogenous lesions.

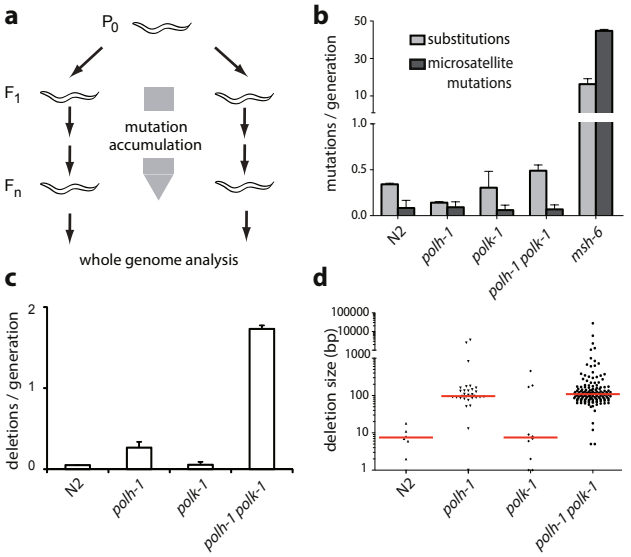

Figure 1. Spontaneous mutagenesis in TLS deficient strains. (A) Generation of mutation accumulation (MA) lines. For each genotype multiple populations were started by cloning out single worms from a single hermaphrodite P0. Cultures were propagated by transferring animals to new plates each generation. At generation Fn, a single animal was grown to a full population of which genomic DNA was isolated and subjected to whole genome sequencing on an Illumina HiSeq. (B) Substitution and microsatellite mutation rates for the indicated genotypes. Mutation rates are expressed as the number of mutations per generation divided by the number of nucleotides analysed. (C) Rates of structural variations for the indicated genotypes. (D) Size distribution of deletions in the different mutant backgrounds. The median sizes are indicated in red.

DSB induction in TLS deficient mutants

To further investigate the origin of the high number of deletions in *polh-1polk-1* deficient strains, we looked for manifestations of genomic instability in germ cells of these animals. We observed a mild but statistically significant increase in the number of foci of the DSB marker RAD-51 in proliferating germ cells of *polh-1polk-1* mutant animals (Figure S3A-B). Elevated levels of DSBs, are also suggested by the spontaneous emergence of dominant *him* mutants in *polh-1polk-1* mutant populations (Figure S1). This phenotype, which is defined by dominant inheritance of an increased number of males (XO) in predominantly hermaphroditic (XX) populations, has previously been found upon exposure to γ-irradiation and in mutants with enhanced telomere shortening, where it proved to result from X/autosome translocations (Herman et al. 1982; Meier et al. 2009). Despite these manifestations of enhanced replication stress in *polh-1polk-1* mutants, the levels of DSBs were insufficient to activate the two DNA damage checkpoints that operate in the *C. elegans* germline: cell cycle arrest and apoptosis (Gartner et al. 2000). We found neither a reduction in germ cell proliferation nor an increase of apoptotic bodies in *polh-1polk-1* mutant germlines, suggesting that TLS compromised germ cells proliferate in the presence of elevated levels of DSBs, with genomic deletions as a consequence (Figure S3C-E).

Footprints of error-prone DSB repair

To obtain mechanistic insight on the biology of deletion formation, we performed a detailed analysis on the sequence context of 141 *polh-1polk-1*-derived deletions (Supplemental data file). While the majority had simple deletion junctions (without inserts), about 25 percent of the footprints showed insertions of short sequence stretches (Figure 2A). Cases with inserts sufficiently long to faithfully trace their origin revealed that the inserted stretch, or part of it, is identical to sequences flanking the deletion (Figure 2B-C). This finding strongly suggests that DNA close to the break site was used as a template for *de novo* synthesis before both DNA ends were joined.

A DSB repair mechanism involving DNA synthesis is also suggested by the notion of a 'priming' nucleotide in more than 80 percent of all deletions: 83 of the 102 deletions without insert contain at the junction at least one nucleotide could have originated from either flank; in 51 cases this is restricted to a single nucleotide. To systematically assess the significance of this observation, we constructed deletion junction heat maps, which reflect the level of (micro)homology between 5' and 3' junctions (Figure 2D-F). We scored the degree of sequence identity in an 8 nt window, encompassing the 4 outermost nucleotides of the flanking sequence and the 4 nucleotides of the adjacent, but deleted, sequence. Indeed, compared to a randomly distributed simulated set, we found a very high similarity score for the nucleotide at the -1 position of the deletions and the +1 position of the opposing flanks ($p=7.3x10^{-17}$). Importantly, this profound degree of microhomology is restricted to only a single, the terminal nucleotide.

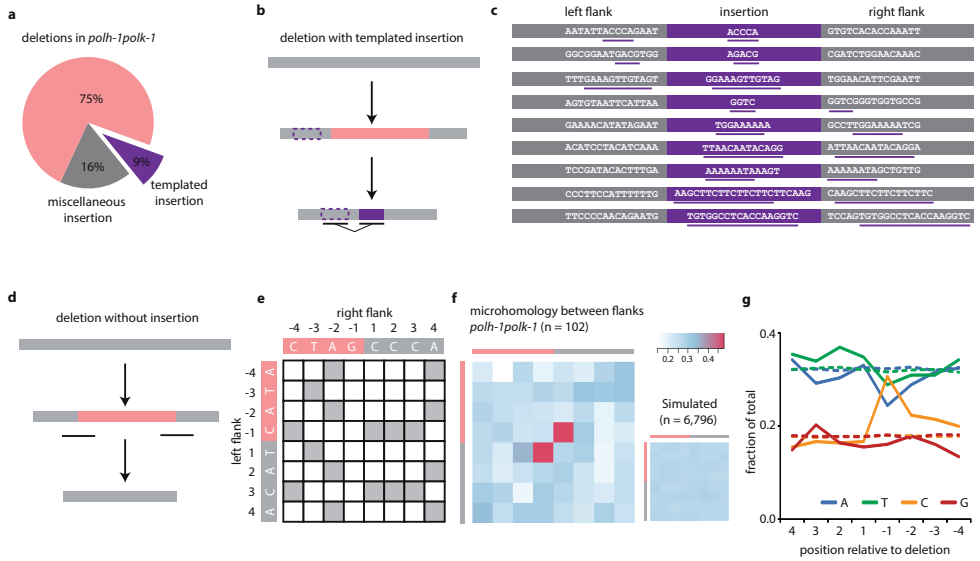

Figure 2. Deletion footprints in TLS mutants indicate a priming-based end joining mechanism. (A) Distribution of deletion footprints in *polh-1polk-1* mutants. (B) Schematic illustration of a deletion associated with a templated insertion. Deleted sequence in pink; newly inserted sequence in purple and its template boxed; non-altered DNA in grey. (C) Sequence context of deletions with templated insertions derived from *polh-1polk-1* animals. Matching sequences are underlined. (D) Schematic illustration of a deletion not accompanied by insertions. Deleted sequence in pink; non-altered DNA in grey. The eight nucleotide window -capturing neighbouring flanking and deleted sequences- that is used for the generation of the heat maps is underlined. (E) The strategy to score junction homology: for each simple deletion, matching bases between the 5′ and 3′ junction were scored 1, non-matching bases were scored 0, thus creating one map per deletion. (F) A heat map representing the sum of all individual deletion maps derived from *polh-1polk-1* animals. (n=102). A heat map for a simulated set of deletions (n=6796) with random distribution is displayed on the right. (G) Base composition at the 5′ and 3′ junctions. The flanking sequences have positive numbers, the deleted sequence have negative; -1 being the first nucleotide within the deletion. Dotted lines indicate the relative abundance of a particular base for a simulated set of deletions (n=6796).

Replication blocking endogenous damage resides at guanines

We next investigated whether the deletion specifics would reveal the nature of the spontaneous damage underlying fork stalling and break formation in TLS compromised animals using the following rationale: deletions in TLS deficient animals are likely brought about because of an inability to incorporate a base across endogenous lesions. If the nascent strand, blocked at the site of base damage, defines one end of the deletion junction, then the -1 position of the corresponding junction will represent the nucleotide complementary to the damaged base: it is the first base not to be incorporated. To test this hypothesis, we plotted the base distribution for each position of the junction and indeed found it not to be random at the -1 position, but rather being dominated by cytosines (Figure 2G). This result strongly argues that spontaneous base damage that requires pol eta and pol kappa to avoid DSB induction resides at guanines, which may point towards N2-dG and/or 8-oxo-dG adducted sites as a primary source of spontaneous mutagenesis.

Deletion formation is dependent on pol theta.

The frequent occurrence of templated insertions at the deletion junctions suggests the involvement

of a DNA polymerase to repair DSBs that are induced at replication-blocking dG bases. One candidate is the A-family DNA polymerase theta, which was previously implicated in repair of interstrand crosslinks in various models and in repair of transposition-induced DSBs in Drosophila (Muzzini et al. 2008; Shima et al. 2004; Yousefzadeh and Wood 2012). We recently identified a role for pol theta in preventing genomic instability at endogenous sequences that are able to fold into potentially replication blocking G-quadruplex structures (Koole et al. 2014). To test a possible role for this protein in deletion formation at spontaneous damage, we generated animals defective for *polh-1polk-1* and the *C. elegans* pol theta homolog *polq-1*. Strikingly, these animals are severely compromised in normal growth: while *polq-1* and *polh-1polk-1* animals had nearly wild-type growth characteristics, *polh-1polk-1polq-1* triple mutant animals had very much reduced fertility, albeit in a stochastic fashion, ranging from complete sterility to brood sizes of 30 percent of wild-type levels (Figure 3A). Associated with these fertility defects, we observed a profound increase in the number of RAD-51 foci in the proliferative zone of the germline as well as activation of the DNA damage checkpoint suggesting increased DNA end-resection and DSB signaling (Figure 3B-C, Figure S3E). From this we conclude that when damage cannot be bypassed, pol theta action safeguards animal fertility by preventing undesired HR-related processing of replication-associated breaks, which trigger checkpoint activation and prohibit proliferation.

Because the notion of endogenous damage blocking the replication fork can only be inferred indirectly from our data, we tested whether a similar detrimental effect of knocking out pol theta is also observed on bona-fide fork-stalling lesions, such as UV-induced photoproducts. Indeed, mutating pol theta strongly sensitizes *polh-1* mutant animals, but not otherwise wild type animals to UV exposure (Figure S3F), further strengthening the conclusion that pol theta action minimizes the toxic effects of persistent replication blocking DNA lesions, that result from either endogenous or exogenous source.

To study the role of pol theta in deletion formation on a molecular level, we assessed mutagenesis using an endogenous *unc-22* reporter gene (Figure 3D). We isolated spontaneous *unc-22* mutants from *polh-1polk-1* and *polh-1polk-1polq-1* populations and determined their molecular nature using PCR and Sanger sequencing. In perfect agreement with our whole-genome sequencing data, all *unc-22* mutations derived from *polh-1polk-1* animals were 50-200 bp deletions characterized by single nucleotide homology and templated insertions (Figure 3D, Table S2). In sharp contrast, *unc-22* mutants derived from *polh-1polk-1polq-1* triple mutants, while being induced at comparable rates, were of a completely different size category. Here, deletions were typically larger than 5 kb, with some spanning over 30 kb of genomic sequence, thus amplifying the deleterious impact of replication stalling lesions more than 100-fold (Figure 3D, Tables S2 and S3). We conclude that a pol theta-mediated end joining mechanism is responsible for the generation of small-sized deletions induced by replication fork stalling endogenous lesions. In its absence, large stretches of DNA surrounding DSBs are resected, resulting in abundant RAD-51 filament formation, mitotic checkpoint activation and excessive loss of DNA.

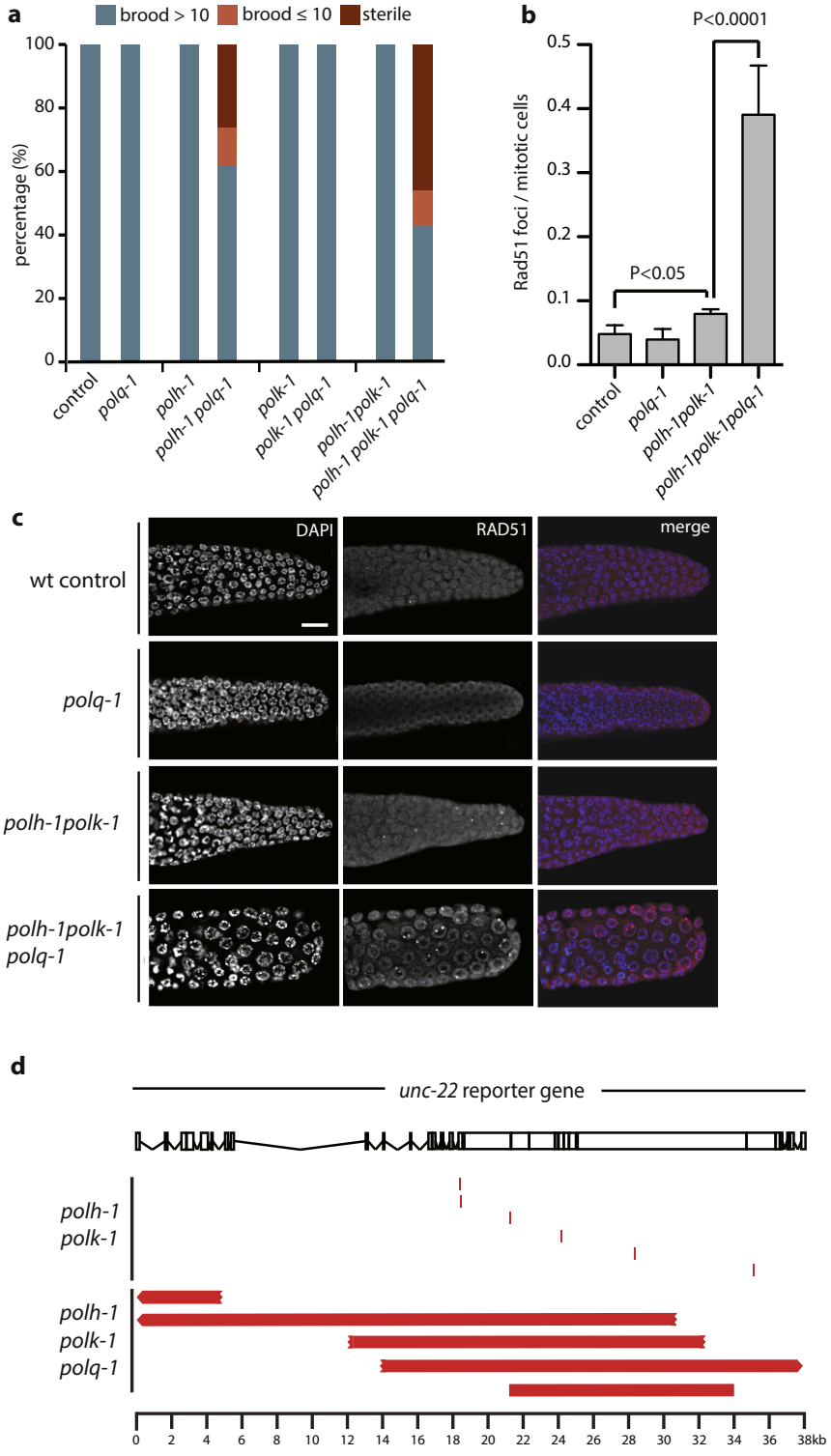
a
brood > 10
brood ≤ 10
sterile
percentage (%)
100
80
60
40
20
0
control
polq-1
polh-1
polh-1 polq-1
polk-1
polk-1 polq-1
polh-1polk-1
polh-1 polk-1 polq-1
b
P<0.0001
P<0.05
Rad51 foci / mitotic cells
0.5
0.4
0.3
0.2
0.1
0.0
control
polq-1
polh-1polk-1
polh-1polk-1polq-1
c
DAPI
RAD51
merge
wt control
polq-1
polh-1polk-1
polh-1polk-1
polq-1
d
unc-22 reporter gene
polh-1
polk-1
polh-1
polk-1
polq-1
0
2
4
6
8
10
12
14
16
18
20
22
24
26
28
30
32
34
36
38kb

Figure 3. Pol theta mediates end joining of breaks in pol eta and pol kappa deficient animals. (A) Fecundity of single, double and triple knockout mutants of pol theta and TLS Polymerases pol eta and pol kappa. (B) Quantification and (C) representative pictures of RAD-51 immunostainings on germlines of the indicated genotype. Scale bar, 10 µm (D) Schematic representation of the *unc-22* reporter gene and spontaneous deletions (in red) isolated from either *polh-1polk-1* or *polh-1polk-1polq-1* mutant animals. Three out of five deletions extended beyond the borders of the *unc-22* locus.

Pol theta in wild-type C. elegans strains

The notion that we have uncovered a role for pol theta in genome protection under TLS deficient conditions raises the question: does pol theta-mediated repair also act when TLS is functional? Or in other words, how relevant is this error-prone repair pathway for animal fitness? We hypothesized that the action of an error-prone repair mechanism with such a clear and distinct signature, *i.e.* a distinct size class, single nucleotide homology and templated insertions, may leave its fingerprint in evolving genomes. For this reason, we compared the genomes of different natural isolates of *C. elegans*, to identify structural variations and defined their characteristics (Figure 4). The majority of deletions are of small size - 60 percent being smaller than 10 bp - while the number of deletions decreases with increasing size in an exponential manner. However, we found deletions in the size range 50-200 bp much more abundantly present than expected from this exponentially declining trend (Figure 4B). Moreover, deletions in this size range bear the pol theta signature: templated insertions and a strong overrepresentation (over 80 percent) of having at least one nucleotide homology (Figure 4C), which supports a role for pol theta in genome change during non-challenged growth. Unexpectedly, we observed templated insertions (2%) also in the small size range of deletions, and found also this class to be dominated by ≥1 nucleotide homology at the junction (Figure 4C-D), hinting to a much broader involvement of pol theta in genomic change, not being restricted to the creation of 50-200 bp deletions.

To further investigate the potential contribution of pol theta in spontaneous mutation induction under non-challenged growth conditions we used a forward mutagenesis assay that is based on the uncoordinated movement of animals carrying a dominant mutation (e1500) in the UNC-93 protein that affects muscle contraction (De Stasio et al. 1997; Greenwald and Horvitz 2003). This phenotype is suppressed by complete loss of function of *unc-93,* or by loss of one of several extragenic suppressor genes (*e.g. sup-9*, *sup-10*). We propagated populations of wild-type and *polq-1* mutant animals out of which we isolated and molecularly characterized revertants animals that had normal movement. Strikingly, the total number of revertants was increased fourfold in *polq-1* mutants (Figure 4E, Tables S4 and S5), demonstrating that pol theta action prevents mutation induction also in wild type animals during normal growth. The increased mutagenesis in *polq-1* is mainly attributed to a selective increase in large chromosomal deletions, similar to those previously identified in *unc-22* in *polh-1polk-1polq-1* deficient strains (Figure S5). Interestingly, we observed that one mutation class, *i.e.* small deletions of a size ≥3 bp, was completely absent in animals *polq-1* (3/28 in wild type vs 0/111 in *polq-1* mutants), arguing, together with the identification of pol theta signature carrying small-sized deletions in the genomes of natural isolates, that pol theta protect cells against arrest and the genome against large chromosomal DNA loss, but at the price of small deletions.

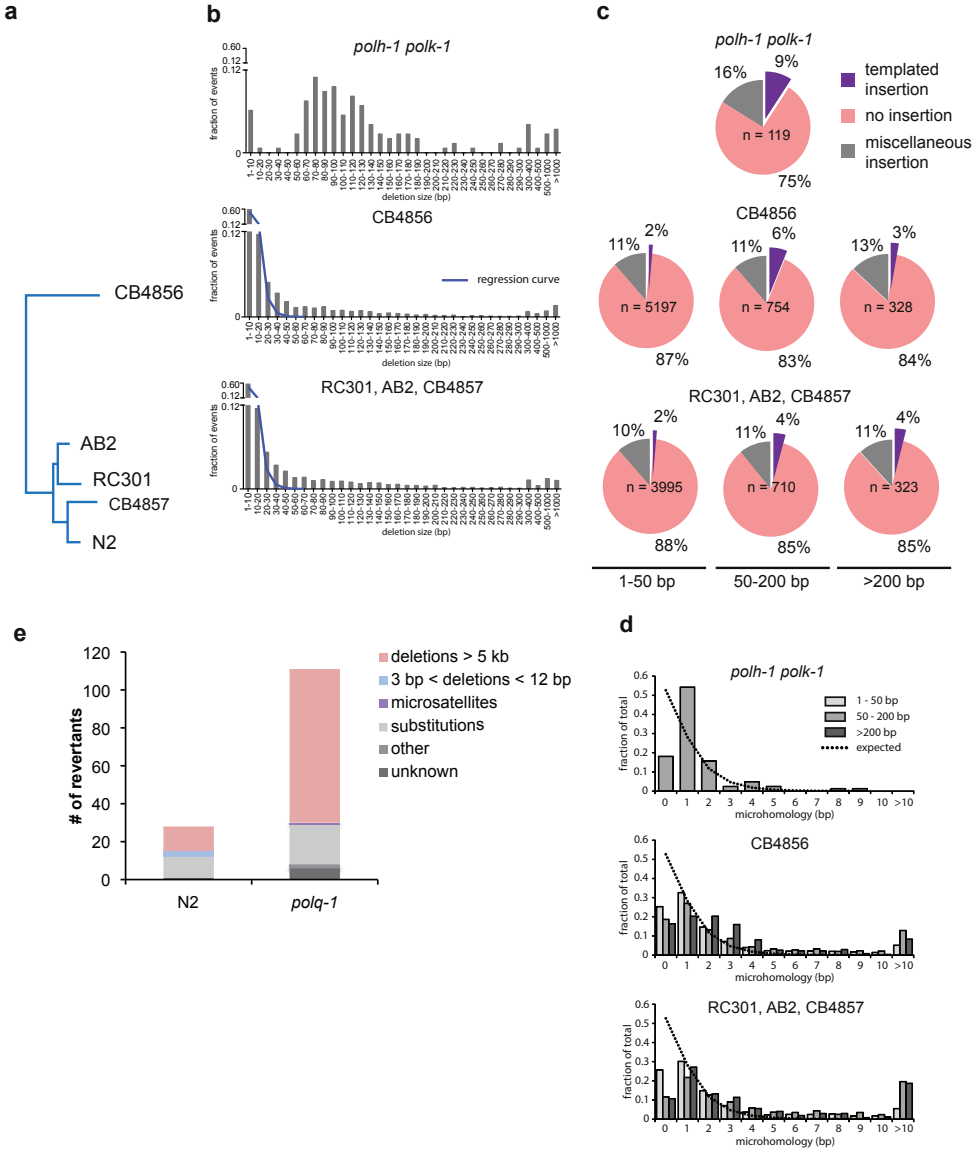

Figure 4. Signature of pol theta-mediated end joining in natural isolates of *C. elegans*. (A) Phylogenetic tree diagram of the different isolates of *C. elegans* used in this study. (B) Size distribution of deletions of evolutionary distinct *C. elegans* species compared to size distribution of *polh-1polk-1* derived deletions. An exponential regression curves describes the size distribution of deletions in both natural isolates up to 20 bp; deletions up to 200 bp are overrepresented. (C) Deletions in natural isolates, especially in size class 50-200 bp show templated insertions analogously to deletion footprints in *polh-1polk-1* animals. (D) Microhomology for deletions in natural isolates as compared to deletions in *polh-1polk-1* animals. (*E*) *unc-93* mutagenesis in *polq-1* worms and wild-type controls.

Discussion

TLS polymerases eta and kappa operate on endogenous lesions in an error free manner

Our data present the first evaluation of the contribution of two main members from the Y family polymerases eta and kappa on the stability of an animal's entire genome under unchallenged conditions. We show that these TLS polymerases prevent the induction of spontaneous deletions. Although *in vitro* studies demonstrated reduced accuracy of pol eta and pol kappa while replicating from undamaged and damaged DNA templates (Johnson et al. 1999; Fischhaber et al. 2002; Masutani et al. 1999a; Matsuda et al. 2000; Kusumoto et al. 2002; Ohashi et al. 2000; Haracska et al. 2000), our *in vivo* data show that the biologically desired bypass action of pol eta and pol kappa is largely error-free: their joined action prevents ~2 deletions per animal generation without significantly affecting the overall substitution rate (Figure 1B).

Deletions were found in animals deficient for pol eta, but not in pol kappa mutant strains. Pol kappa nevertheless can act on spontaneous damage as a greatly increased number of deletions result from the combined absence of both pol eta and pol kappa. This outcome argues that the two Y-family members function redundantly on a subset of endogenous lesions, a conclusion that is further supported by a similar genetic interaction for sensitivity towards the guanine alkylator MMS. Also for this exogenous source of DNA damage, animals deficient for both pol eta and pol kappa are profoundly more sensitive than animals deficient for only pol eta, while pol kappa disruption by itself only very mildly increases the sensitivity of wild-type worms. (Roerink et al. 2012). Under non-challenged conditions, we found deletion junctions to preferentially result from replication fork stalling at dG residues (Figure 2G), which may point towards N2-dG and/or 8-oxo-dG adducted sites as a primary source of spontaneous mutagenesis, as bypass activities of pol eta and pol kappa have been reported for these lesions (Avkin et al. 2004; Haracska et al. 2000).

An error-prone pol theta-mediated mechanism for repair of replication-associated DSBs

The footprints of the deletions that are suppressed by TLS polymerases fit best with a model in which one end of a DSB, induced at replication-blocking lesions, is extended using the other end as a template, with just a single base-paired nucleotide as a primer (explaining both single nucleotide homology and templated insertions). In this model, templated inserts can be explained as the result of iterative rounds of annealing and extension (Figure 5). The close proximity of insertions to their template also suggests that the extendable end of the DSB is not subjected to extensive trimming and suggests that DNA close to the break site was used as a template for *de novo* synthesis before both DNA ends were joined. A 'priming' nucleotide in more than 80 percent of all deletions further strengthened our hypothesized model of a DSB repair mechanism involving DNA synthesis. Further support is provided by the identification of a polymerase, the A-family polymerase pol theta, which we found to be essential for the formation of small-sized deletions. The molecular function of this protein in previously identified phenotypes, such as sensitivity towards crosslinking agents and radiation, as well as spontaneous genome instability in mice was largely unknown (Muzzini et al. 2008; Shima et al. 2004; Yousefzadeh and Wood 2012). We now show that a pol theta-dependent repair route provides cells with the ability to repair replication-associated breaks; we propose to refer to this pathway as TMEJ, for Pol Theta-Mediated End Joining, to set it apart from canonical NHEJ. We hypothesize that TMEJ may be specifically important in cases where the sister chromatid cannot be used as a DSB repair template for *e.g.* homologous recombination because that template still contains the original replication-blocking lesion (Figure

5). In favor of a role of TMEJ in preventing futile HR, we observed abundant RAD-51 filament formation, mitotic checkpoint activation and excessive loss of DNA in the absence of pol theta. When damage cannot be bypassed, pol theta action safeguards animal fertility by preventing undesired HR-related processing of replication-associated breaks, which would trigger checkpoint activation and prohibit proliferation.

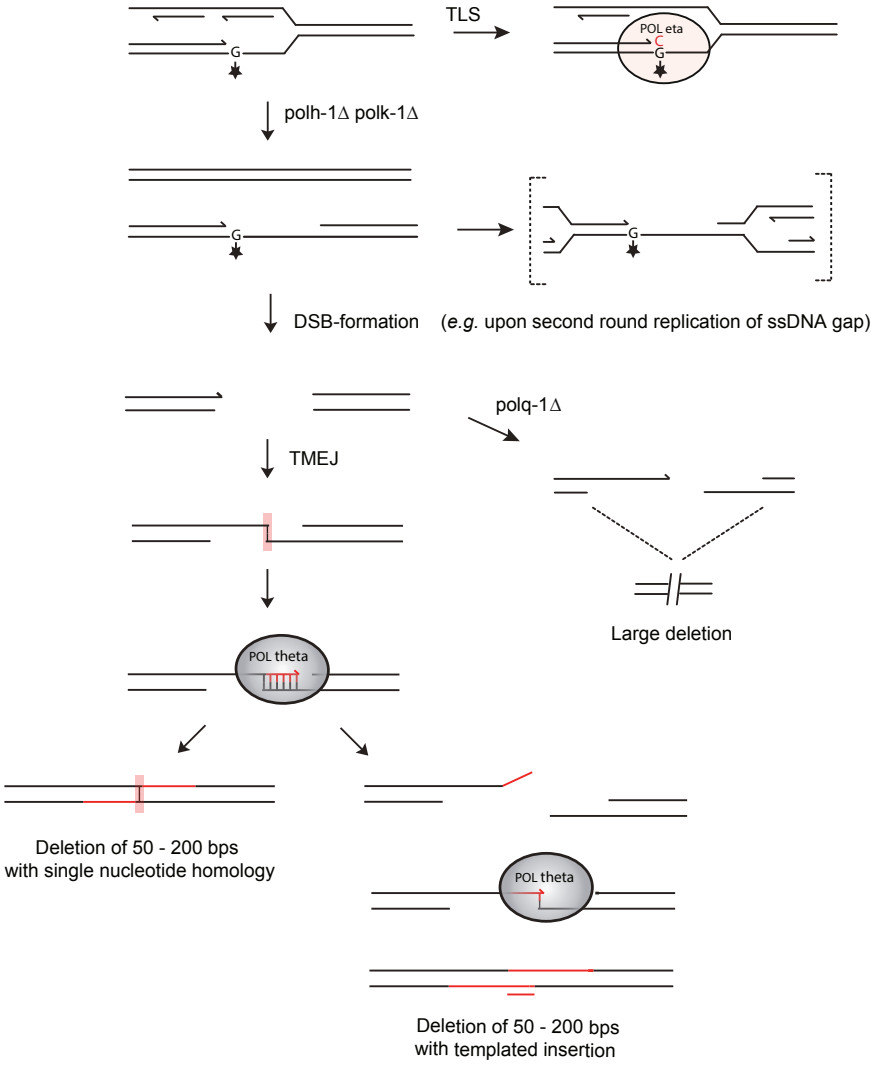

Figure 5. A tentative model for TMEJ of breaks induced at replication fork barriers. DNA lesions from endogenous sources - with increased frequency in the absence of functional TLS - causes replication fork blocks, leading to double stranded breaks. The broken ends are repaired by pol Theta-Mediated End Joining (TMEJ), which is stimulated by minimal priming of 1 base pair, explaining deletions with single nucleotide homology (left). Iterative cycles of priming, extending and dissociation will result in deletions with templated insertions (right). In pol theta deficient cells, DNA breaks resulting from replication fork stalling are differently processed, eventually leading to deletions of larger size.

Our model for TMEJ is conceptually different from the models that have previously been proposed to explain copy number variations and complex rearrangements in tumors and congenital disorders: microhomology-mediated break induced replication (MMBIR), and Fork stalling and Template switching (FoSTeS) (Hastings et al. 2009; Lee et al. 2007; Zhang et al. 2001). The genome rearrangements explained by these models are also characterized by the presence of limited sequence homology at the rearranged DNA junctions, however, both these models invoke the invasion of a 3' single strand end, either resulting from DNA breaks (MMBIR), or stalled forks (FoSTes) into the sister molecule or into another replication fork that is in 3D physical proximity, to reassure ongoing DNA replication. Our data on deletion junctions that result from blocked replication either at endogenous lesions (this manuscript) or secondary structures such as G4 DNA (Koole et al. 2014) favor an end-joining mechanism based on the presence of two-ended double strand breaks - which may be the result from replication of gapped DNA intermediates that form at persistent replication fork blocks (Figure 5) - as opposed to restarting replication of a one-ended break. The observation that Mus308, the Drosophila ortholog of pol theta, can act on dsDNA breaks resulting from P-element excision, is also in concert with an end-joining mechanism.

Another difference between TMEJ and MMBIR/FoSTeS relates to size; whereas TMEJ deletions are typically 50-200, the rearrangements that are explained by MMBIR/FoSTeS models span kilobases. Nevertheless, all models evoke the presence of flexible primer-template intermediates that can be extended in recurrent cycles, and imply DNA polymerase action. Important in that respect is the recent observation that MMBIR-type rearrangement in mammalian cells can be induced by replication stress and depend at least in part on the Pol delta subunit PolD4 (Costantino et al. 2014).

Of interest, while the vast majority of genomic rearrangements that we observed in TLS compromised animals are 50-200 deletions, we nevertheless found a very small number of more complex rearrangements (Supplemental data file). These events may, because of their complexity and size, be more resembling the complex rearrangement found in mammalian cells, however, their number was too limited to allow systematic analyses, and none were found in any of our other less sensitive phenotype-based assays, thus precluding genetic analysis at this stage.

TMEJ footprints in evolving genomes

The observation that pol theta also suppresses mutagenesis in wild-type animals, together with the notion that the signature of TMEJ is apparent in the genomes of natural isolates of *C. elegans* argues for a prominent role of this error-prone pathway to protect genomes against large chromosomal rearrangements. This role seems not to be restricted to replication fork stalls. While the class of 50-200 bp deletions that is seen in TLS deficient animals, is found overrepresented in genomes of natural isolates, the predominant fraction of deletions are smaller in size. Still, these smaller-sized deletions bear a TMEJ signature, in that they are characterized by single nucleotide homology and frequently are associated with templated insertions. A broader role for TMEJ, thus being responsible for many types of structural variations, is also supported by the *unc-93* forward mutagenesis assay, where small deletions (3 to 12 bp) were exclusively found in pol theta-proficient strains.

While mutagenic processes are drivers of evolution, they also fuel malignant transformation of cells. It is a current challenge to recognize specific classes of mutations in cancer genomes and attribute these either to underlying sources of DNA damage or to error-prone repair mechanisms. Identifying mutational signatures typifying specific repair processes is pivotal to this ambition.

Templated insertions and the use of minimal homology - two characteristics of TMEJ - have frequently been observed in higher order eukaryotes and in cancer tissues (Chen et al. 2010; Nik-Zainal et al. 2012; Carvalho et al. 2013), and have been ascribed to either classical non-homologous end joining or the molecularly ill-defined process of microhomology-mediated end joining (Honma et al. 2007; Kloosterman et al. 2012). Here, we describe a mechanistic alternative for repair of DSBs induced at stalled forks, which leaves a distinct and well-defined footprint in evolving genomes.

Methods

C. elegans genetics

All strains were cultured according to standard methods (Brenner 1974). Wild-type N2 (Bristol) worms were used in all control experiments. Alleles used in this study are: *polh-1 (lf31)*; *polh-1 (ok3317)*; *polk-1 (lf29)*; *polq-1(tm2026); msh-6(pk2504)*; *bcIs39[P(lim-7)ced-1::GFP + lin-15(+)]); unc-93(e1500)*. All mutant strains were backcrossed six times before performing experiments.

Whole genome sequencing of MA lines

Mutation accumulation (MA) lines were generated by cloning out F1 animals from one hermaphrodite. Each generation about five worms were transferred to new plates. MA lines were maintained for 60 generations or until severe growth defects developed. Single animals were then cloned out and propagated to obtain full plates for DNA isolation. Worms were washed off with M9 and incubated for one hour at room temperature while shaking, to remove bacteria from the animal's intestine. After two washes, worm pellets were lysed for two hours at 65°C with SDS containing lysis buffer. Genomic DNA was purified by using a DNeasy kit (Qiagen). Paired end (PE) libraries for whole genome sequencing (HiSeq2000 Illumina) were constructed from genomic DNA according to manufacturers' protocols with some adaptations. Shortly, 5 g DNA was sheared using a Covaris S220 ultrasonicator, followed by DNA end-repair, formation of 3'A overhangs using Klenow and ligation to Illumina PE adapters. Adapter-ligated products were purified on QIAquick spin columns (Qiagen) and PCR-amplified using Phusion DNA polymerase and barcoded Illumina PE primers for 10 cycles. PCR products of the 300 - 400 bp size range were selected on a 2% ultrapure agarose gel and purified on Qiaquick spin columns. DNA quality was assessed and quantified using an Agilent DNA 1000 assay. Four to five barcoded libraries were pooled in one lane for sequencing on a HiSeq.

Bioinformatic analysis

Image analysis, basecalling and error calibration was performed using standard Illumina software. For the analysis of the natural isolates paired-end whole genome sequence data was downloaded from the NCBI Sequence Read Archive (SRP011413) (Grishkevich et al. 2012), and sequence reads were mapped to the *C. elegans* reference genome (Wormbase release 225) by BWA. SAMtools was used for SNP and indel calling, with BAQ calculation turned off (Li et al. 2009). All non-unique SNPs and indels are considered to be pre-existing and were filtered out using custom Perl scripts. To identify microsatellite mutations and deletions we used Pindel, developed by Ye et al (Ye et al. 2009). A more detailed description of the bioinformatic procedures is enclosed in the supplemental information.

Microscopy

To study RAD-51 foci formation, germlines were dissected, freeze cracked and subsequently washed with 1% Triton and methanol (-20°C). RAD-51 was visualized by using an anti-RAD-51 rabbit monoclonal antibody and an Alexa488-labelled goat-anti-rabbit secondary antibody (Molecular Probes Inc), combined with 10 μg/mL DAPI. Dissected worms and eggs were mounted using Vectashield. Apoptosis was monitored using a *lim-7* driven *CED-1*::GFP fusion, which visualises sheath cells surrounding apoptotic germ cells. All microscopy was performed with a Leica DM6000 microscope.

UV sensitivity assay

To assess the sensitivity to germ cells to UV-exposure, young adults were exposed to various doses of UV light, and subsequently allowed to lay eggs for 48 hrs. 24 hrs later, the number of non-hatched eggs and surviving progeny were determined.

unc-22 mutagenesis assay

To identify spontaneous mutations in the *unc-22* muscle gene we started 50 populations by transferring a single animal to 9 cm plates seeded with OP50. In the case of the synthetically sick *polh-1polk-1polq-1* mutant, we started 200 populations with 5 worms per plate. Animals were washed off with 2 mM levamisole and transferred to 6-well plates to facilitate scoring of *unc-22* mutants, which are insensitive to the hypercontracting effects of the drug levamisole. Independent *unc-22* mutant animals were isolated. Genomic DNA was isolated from homozygous animals for subsequent PCR and sequence analysis.

unc-93 (e1500) mutagenesis assay

To generate a complete spectrum of spontaneous mutations we used a mutagenesis assay based on reversion of the socalled 'rubber band' phenotype, caused by a dominant mutation in the muscle gene *unc-93* (De Stasio et al. 1997; Greenwald and Horvitz 2003). Reversion of the *unc-93(e1500)* phenotype is caused by homozygous loss of *unc-93* or one of the suppressor genes *sup-9*, *sup-10*, *sup-11* and *sup-18*. *polq-1(tm2026) unc-93(e1500)* and *unc-93(e1500)* animals were singled to 2 x 400 6 cm plates. These plates were grown till starvation and equal fractions (chunks of 2 x 2 cm) were then transferred to 9 cm plates. Before these plates were fully grown, they were inspected for wild-type moving animals. From each starting culture only one revertant animal was isolated to ensure independent events.

Large chromosomal deletions in *unc-93*, *sup-9* and *sup-10* were identified by PCR amplification of exonic regions and two regions 5 kb upstream and downstream of the respective genes. Smaller genetic changes and substitutions were first classified into events in either the *unc-93* gene or in one of the suppressor genes by their ability to complement a known *unc-93* deletion allele. All *unc-93* exons were sequenced in revertant animals that failed to complement *unc-93*, whereas all exons of *sup-9* and *sup-10* were sequenced in revertants that complemented *unc-93*. *sup-11* or *sup-18* could not be subjected to molecular analysis due to lack of sequence data. Revertants that complemented *unc-93* but had not detectable mutation of *sup-9* or *sup-10*, were classified as 'unknown'.

Data access

The sequencing data have been submitted to the NCBI Sequence Read Archive under accession number SRP020555. For the analysis of the natural isolates, paired-end whole genome sequence

data was downloaded from the NCBI Sequence Read Archive (SRP011413) (Grishkevich et al. 2012).

Acknowledgements

We thank the *C. elegans* Knockout Consortium, Shohei Mitani and the C. elegans Genetics Center for providing strains. We thank Wouter Koole and Jane van Heteren for critical reading of the manuscript and Bennie Lemmens and Harry Vrieling for discussions. MT is supported by grants from the European Research Council (203379, DSBrepair) and ZonMW/NGI-Horizon, Zenith.

a

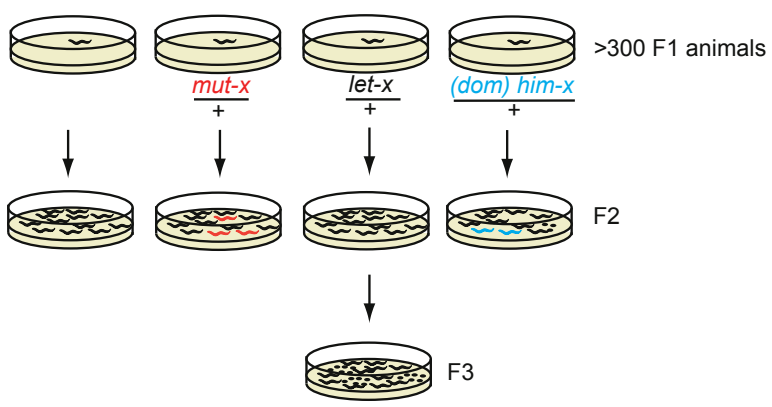

b

Genotype	# analyzed plates	Mutants found
N2	340	0
polh-1(ok3317)	340	0
polh-1(lf31)	340	0
polk-1(lf29)	340	0
polh-1(ok3317);polk-1(lf29)	740	*dpy(3); ste(1); let(15); him(6)*
polh-1(lf31);polk-1(lf29)	340	*dpy(3); let(5); him(3)*
msh-6	300	20 visible mutants

Figure S1. Occurrence of spontaneous visible mutants in TLS defective strains. a, Experimental set-up to determine spontaneous mutagenesis: the F1 brood of non-mutant segregating hermaphrodites (P0) were singled to establish individual populations. These were inspected for mendelian segregation of abnormal phenotypes indicating the occurrence of a recessive mutations in the gametes of the P0. Mutants affecting body morphology (e.g. dumpy/dpy) or movement (i.e. uncoordinated/unc) can be scored in the F2 progeny. Mutations in essential genes (i.e. lethal/let) give rise to islands of dead eggs when populations are allowed to clear the food supply. Elevated numbers of males in the F2 progeny indicate a high incidence of males (him) phenotype, arguing for a dominant him mutation in the F1. b, Quantification of visible mutant phenotypes. The data for *msh-6* mutants have been published previously.

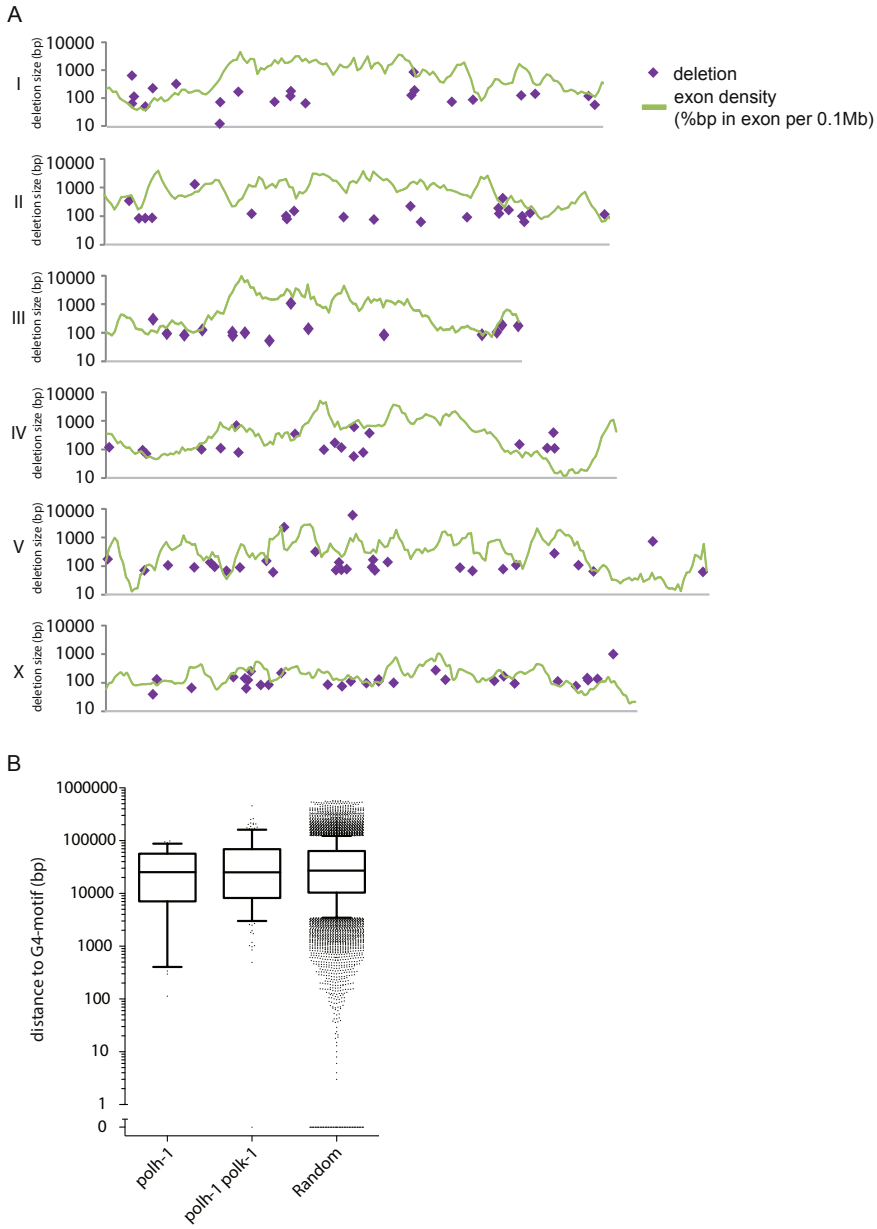

Figure S2. Genomic distribution of deletions in *polh-1polk-1* mutant animals. (A) Individual deletions (purple) were plotted onto a physical map of the C. elegans genome. The y-axis shows the size of the deletion on a logarithmic scale. The exon density is displayed in green (y-axis not shown). The length of the graph shows the size of the indicated chromosome relative to each other. (B) For each individual deletion the distance to the closest G4-motif G3-5N1-5G3-5N1-5G3-5N1-5G3-5 (1680 G4-motifs are present in the *C. elegans* genome) was determined. A random set of ~13,000 deletions with a size distribution similar to those observed in *polh-1 polk-1* mutants was plotted as a comparison. No statistical difference was found betweenthis random set and the set obtained from *polh-1* or *polh-1 polk-1* double mutant animals. Whiskers are drawn down to the 10th percentile and up to the 90th percentile. A distance of zero means that the nearest G4 motif is within the deletion.

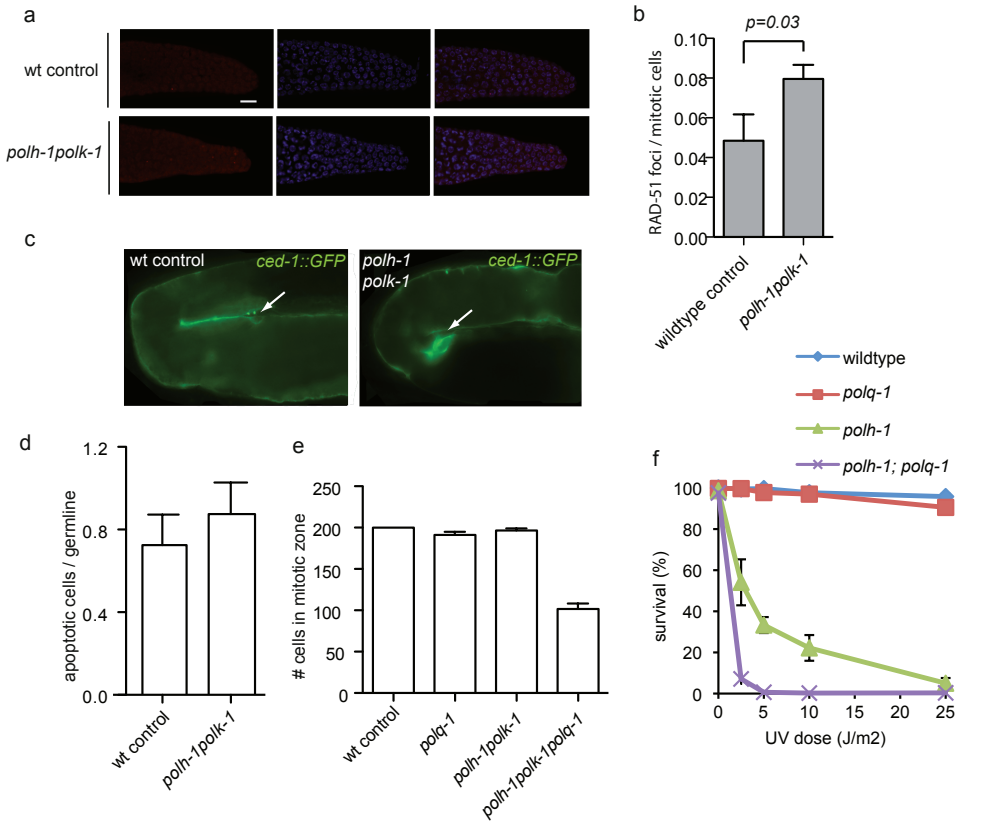

Figure S3. Analysis of DNA damage induction and apoptosis in single, double and triple mutants of *polh-1*, *polk-1* and *polq-1*. a. Representative images and b. quantification of RAD-51 foci for theindicated genotypes in nuclei present in the proliferative compartment of the *C. elegans* reproductivesystem. DAPI stainings in blue, RAD-51 in red. Scale bar, 10 µm c. Representative images of the bend ofthe gonad arm of animals transgenic for the apoptotic marker ced-1::GFP; cells in the process of apoptotic engulfment are indicated with arrows. Scale bar, 10 µm d. Quantification of apoptotic cells in *polh-1polk-1* mutant animals and wild-type controls. e. Quantification of the number of nuclei in themitotic region of the germline. A reduction in the number of cells in this region is an establishedoutcome of checkpoint activation. f. Sensitivity of *polh-1* and *polq-1* single and double mutants for exposure to UV, plotted as the fraction of surviving progeny after germline exposure of young adult worms.

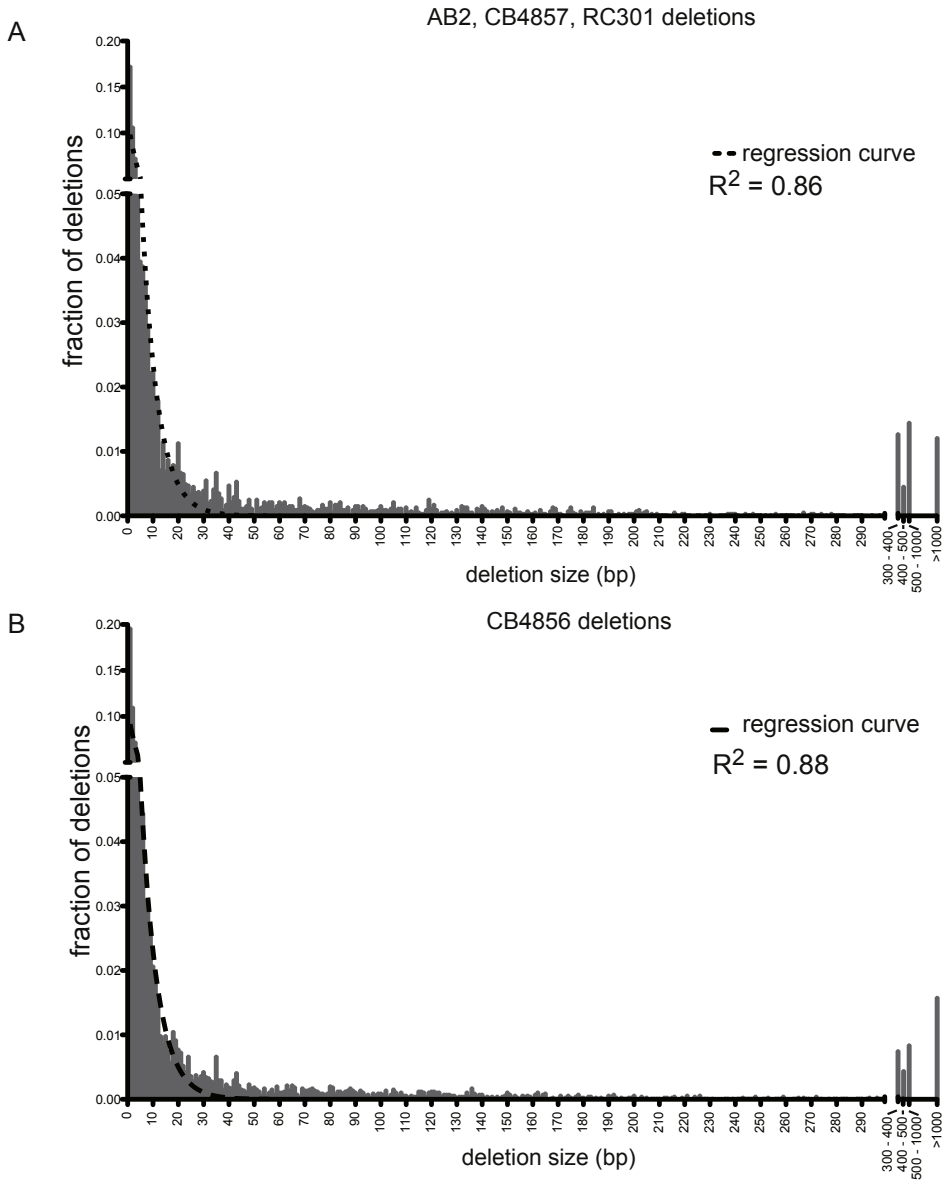

Figure S4. Histogram of size distributions is plotted of the various *C. elegans* natural isolates that were analyzed. Regression analysis showed that an exponential fit for deletion sizes up to 20bp approaches the actual distribution best. (A) the grouped distribution for AB2, CB4857 and RC301. (B) as in (A), but now for CB4856.

A

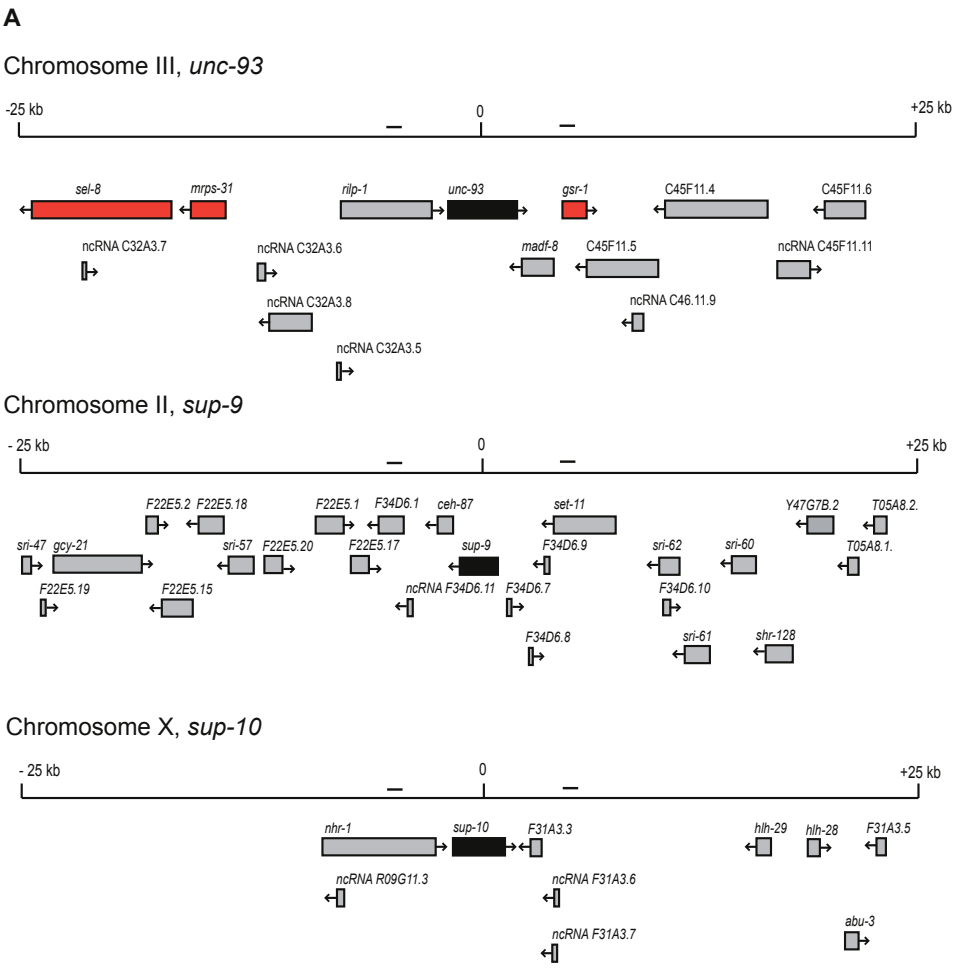

B

	unc-93	*sup-9*	*sup-10*
wildtype	0	2	11
polq-1	6	20	55

Figure S5. Selective occurence of large chromosomal deletions in regions that are devoid of essential genes in the *unc-93* mutagenesis assay. (A) Schematic representation of 50 kb regions surrounding the *unc-93*, *sup-9* and *sup-10* genes. Known essential genes are depicted in red. While *unc-93* is flanked by two essential genes, no essential genes are known in the 50 kb intervals around *sup-9* and *sup-10*. To estimate deletion sizes, amplification of PCR products at -5kb and +5kb positions has been tested. (B) Number of deletions larger than 5kb in *unc-93*, *sup-9* and *sup-10*.

Table S1. Whole genome sequencing statistics.

genotype	sample	# generations	# reads	average coverage	# bp >= 4x covered
N2	N2	60	45,258,326	28x	100,140,732
	N4	60	23,693,826	16x	99,675,920
polh-1(lf31)	H7	60	46,203,688	39x	100,229,062
	H8	60	44,982,616	37x	100,238,324
polk-1(lf29)	K1	60	41,517,548	21x	99,970,233
	K4	60	39,275,458	30x	100,235,635
	K9	60	40,037,564	24x	100,120,773
polh-1(lf31);polk-1(lf29)	D4	32	46,284,780	21x	99,911,564
	D13	25	38,712,292	29x	100,224,845
	D14	25	59,163,976	27x	100,202,641
msh-6 (pk2504)	M13	10	48,338,722	19x	99,236,278
	M15	10	44,129,942	12x	99,799,729

Table S2. unc-22 deletions in *polh-1polk-1* and *polh-1polk-1polq-1*.

	size	left flank	deletion left	deletion right	right flank	insertion
polh-1polk-1						
A	83 bp	GTACCTACTCA	CGTCCAAATG	TTATCGAAAA	GAACGTGTGC	–
B	74 bp	AATCCAGAAGT	CGATGACACC	CTTGGTTAGT	TATTTTTTGG	–
C	153 bp	ACAAGGCTGGG	CCTGGACAAC	TAAAGGCTGG	AGCCACTGTT	–
D	119 bp	GACTATCAAGG	CTGGTCAATC	TGATAACCCA	GAATACCAAT	AATCTGACTATCAAAGGAAATCTCAA-GAATCTGACTATCAAAG
E	93 bp	CTTGCAAAGGA	TCCATTTGGA	CACGTGACAA	CGGTGGATCA	–
F	71 bp	TGTGAAGCCTT	ACGGAACTGA	ACCACCAGTT	GTTACTTGGC	–
G		not identified				
polh-1polk-1 polq-1						
A	>4.7 kb					
B	>30.5 kb					
C	19 - 20.6 kb					
D	12660 bp	AAATGAGCACA	CTATTCTGTG	GAACAGGAGC	ATTTGGAGTT	
E	> 23.7 kb					
F		not identified				

Table S3. Frequency of *unc-22* mutations in *polq-1*, *polh-1polk-1* and *polh-1polk-1polq-1*.

Strain		total # plates scored	# plates containing one or more twitchers	estimated mutation rate
N2	wild-type	40	0	0.00E+00
XF152	*polq-1*	40	0	0.00E+00
XF507	*polh-1polk-1*	46	7	8.00E-06
XF840	*polh-1polq-1polk-1*	39	6	8.00E-06

Table S4. Sequence analysis of reversion mutants for *unc-93(e1500)*.

wild-type			
unc-93			
deletions > 5kb	0		
substitutions	6	cagttt(g>a)tctggc; C>Y	
		gacacg(t>a)cacagt; V>D	
		tgtctg(g>c)aatact; G>A	
		aaatat(c>t)gatttt; R>L	
		ggaatc(g>a)cggctt; T>A	
		tgttag(g>t)taatgg; splice	
other	1	gaatat(tcga>deleted)aaaactt	3bp > deletion > 12 bp
sup-9			
deletions > 5kb	2		
substitutions	1	ccattg(g>a)gactta; G>stop	
other	2	ccaata(gtga>deleted)cgtcat	3bp > deletion > 12 bp
		tctgta(ccgggtgggga>deleted)ggtctg	3bp > deletion > 12 bp
sup-10			
deletions > 5kb	11		
substitutions	3	cagttc(t>a)cttgta; L>H	
		tggaat(a>g)tggtcgg; M>V*	
		agccag(g>t)tttgta;; splice site mutation	
unknown	2		

*also tctttt(t>c)caacca in intron 150 bp upstream

Table S5. Sequence analysis of reversion mutants for *polq-1; unc-93(e1500)*.

polq-1			
unc-93			
deletions > 5kb	6		
substitutions	12	tgcgga(c>a)aagtcg; Q>K	
		cgttga(c>a)gattttc; T>K	
		gatctc(g>a)gatctg; G>R	
		ttccat(c>t)atttat; S>L	
		tttcta(c>a)ctcatg; T>N	
		tttcat(g>t)attgta; M>I	
		ggggag(c>a)caaatg; A>D	
		aagtcg(t>a)cggaaa; V>D	
		tccttt(c>t)gagaca; R>stop	
		tctata(c>a)attgtc; Y>stop	
		aatata(t>a)ttgctg; Y>stop	
		tgttag(g>a)taatgg; splice site mutation	
other	2	acgtca(ca>deleted)gttgaa	other
		ttttac(t>deleted)ttttag	microsatellite
sup-9			
deletions > 5kb	20		
substitutions	7	tcttcg(g>a)gctcac; G>E	
		gggtac(c>a)agtgga; Q>K	
		gtggag(c>a)atttta; A>E	
		ccattg(g>a)gactta; G>stop	
		aggcta(c>a)ggtcat; Y>stop	
		tccctg(c>t)aaactc; Q>stop	
		caagta(c>a)aacatg; Y>stop	
sup-10			
deletions > 5kb	55		
substitutions	1	atgtta(a>t)tataag; N>I	
other	1	gtgatg(a>deleted)catcaa	hairpin
unknown	7		

REFERENCES

Avkin S, Goldsmith M, Velasco-Miguel S, Geacintov N, Friedberg EC, Livneh Z. 2004. Quantitative analysis of translesion DNA synthesis across a benzo[a]pyrene-guanine adduct in mammalian cells: the role of DNA polymerase kappa. *J Biol Chem 279*: 53298–53305.

Brenner S. 1974. The genetics of Caenorhabditis elegans. *Genetics 77*: 71–94.

Carvalho CMB, Pehlivan D, Ramocki MB, Fang P, Alleva B, Franco LM, Belmont JW, Hastings PJ, Lupski JR. 2013. Replicative mechanisms for CNV formation are error prone. *Nat Genet*.

Chen J-M, Cooper DN, Férec C, Kehrer-Sawatzki H, Patrinos GP. 2010. Genomic rearrangements in inherited disease and cancer. *Semin Cancer Biol 20*: 222–233.

Costantino L, Sotiriou SK, Rantala JK, Magin S, Mladenov E, Helleday T, Haber JE, Iliakis G, Kallioniemi OP, Halazonetis TD. 2014. Break-induced replication repair of damaged forks induces genomic duplications in human cells. *Science 343*: 88–91.

De Stasio E, Lephoto C, Azuma L, Holst C, Stanislaus D, Uttam J. 1997. Characterization of revertants of unc-93(e1500) in Caenorhabditis elegans induced by N-ethyl-N-nitrosourea. *Genetics 147*: 597–608.

Fischhaber PL, Gerlach VL, Feaver WJ, Hatahet Z, Wallace SS, Friedberg EC. 2002. Human DNA polymerase kappa bypasses and extends beyond thymine glycols during translesion synthesis in vitro, preferentially incorporating correct nucleotides. *J Biol Chem 277*: 37604–37611.

Gartner A, Milstein S, Ahmed S, Hodgkin J, Hengartner MO. 2000. A conserved checkpoint pathway mediates DNA damage--induced apoptosis and cell cycle arrest in C. elegans. *Mol Cell 5*: 435–443.

Greenwald IS, Horvitz HR. 2003. unc-93(e1500): A behavioral mutant of Caenorhabditis elegans that defines a gene with a wild-type null phenotype. *Genetics 96*: 147–164.

Grishkevich V, Ben-Elazar S, Hashimshony T, Schott DH, Hunter CP, Yanai I. 2012. A genomic bias for genotype-environment interactions in C. elegans. *Mol Syst Biol 8*: 587.

Haracska L, Yu SL, Johnson RE, Prakash L, Prakash S. 2000. Efficient and accurate replication in the presence of 7,8-dihydro-8-oxoguanine by DNA polymerase eta. *Nat Genet 25*: 458–461.

Hastings PJ, Ira G, Lupski JR. 2009. A microhomology-mediated break-induced replication model for the origin of human copy number variation. *PLoS Genet 5*: e1000327.

Herman RK, Kari CK, Hartman PS. 1982. Dominant X-chromosome nondisjunction mutants of Caenorhabditis elegans. *Genetics 102*: 379–400.

Honma M, Sakuraba M, Koizumi T, Takashima Y, Sakamoto H, Hayashi M. 2007. Non-homologous end-joining for repairing I-SceI-induced DNA double strand breaks in human cells. *DNA Repair 6*: 781–788.

Johnson RE, Prakash S, Prakash L. 1999. Efficient bypass of a thymine-thymine dimer by yeast DNA polymerase, Poleta. *Science 283*: 1001–1004.

Johnson RE, Yu S-L, Prakash S, Prakash L. 2007. A role for yeast and human translesion synthesis DNA polymerases in promoting replication through 3-methyl adenine. *Mol Cell Biol 27*: 7198–7205.

Kloosterman WP, Tavakoli-Yaraki M, van Roosmalen MJ, van Binsbergen E, Renkens I, Duran K, Ballarati L, Vergult S, Giardino D, Hansson K, et al. 2012. Constitutional chromothripsis rearrangements involve clustered double-stranded DNA breaks and nonhomologous repair mechanisms. *CellReports 1*: 648–655.

Knobel PA, Marti TM. 2011. Translesion DNA synthesis in the context of cancer research. *Cancer Cell Int 11*: 39.

Koole W, van Schendel R, Karambelas AE, van Heteren JT, Okihara KL, Tijsterman M. 2014. A Polymerase Theta-dependent repair pathway suppresses extensive genomic instability at endogenous G4 DNA sites. *Nat Commun 5*.

Kusumoto R, Masutani C, Iwai S, Hanaoka F. 2002. Translesion synthesis by human DNA polymerase eta across thymine glycol lesions. *Biochemistry 41*: 6090–6099.

Lee JA, Carvalho CMB, Lupski JR. 2007. A DNA replication mechanism for generating nonrecurrent rearrangements associated with genomic disorders. *Cell 131*: 1235–1247.

Li H, Handsaker B, Wysoker A, Fennell T, Ruan J, Homer N, Marth G, Abecasis G, Durbin R, 1000 Genome Project Data Processing Subgroup. 2009. The Sequence Alignment/Map format and SAMtools. *Bioinformatics 25*: 2078–2079.

Lynch M. 2008. The cellular, developmental and population-genetic determinants of mutation-rate evolution. *Genetics 180*: 933–943.

Masutani C, Araki M, Yamada A, Kusumoto R, Nogimori T, Maekawa T, Iwai S, Hanaoka F. 1999a. Xeroderma pigmentosum variant (XP-V) correcting protein from HeLa cells has a thymine dimer bypass DNA polymerase activity. *EMBO J 18*: 3491–3501.

Masutani C, Kusumoto R, Yamada A, Dohmae N, Yokoi M, Yuasa M, Araki M, Iwai S, Takio K, Hanaoka F. 1999b. The XPV (xeroderma pigmentosum variant) gene encodes human DNA polymerase

eta. *Nature 399*: 700–704.
Matsuda T, Bebenek K, Masutani C, Hanaoka F, Kunkel TA. 2000. Low fidelity DNA synthesis by human DNA polymerase-eta. *Nature 404*: 1011–1013.
Meier B, Barber LJ, Liu Y, Shtessel L, Boulton SJ, Gartner A, Ahmed S. 2009. The MRT-1 nuclease is required for DNA crosslink repair and telomerase activity in vivo in Caenorhabditis elegans. *EMBO J 28*: 3549–3563.
Mitelman F, Johansson B, Mertens F. 2007. The impact of translocations and gene fusions on cancer causation. *Nat Rev Cancer 7*: 233–245.
Muzzini DM, Plevani P, Boulton SJ, Cassata G, Marini F. 2008. Caenorhabditis elegans POLQ-1 and HEL-308 function in two distinct DNA interstrand cross-link repair pathways. *DNA Repair 7*: 941–950.
Nik-Zainal S, Alexandrov LB, Wedge DC, Van Loo P, Greenman CD, Raine K, Jones D, Hinton J, Marshall J, Stebbings LA, et al. 2012. Mutational Processes Molding the Genomes of 21 Breast Cancers. *Cell 149*: 979–993.
Ohashi E, Bebenek K, Matsuda T, Feaver WJ, Gerlach VL, Friedberg EC, Ohmori H, Kunkel TA. 2000. Fidelity and processivity of DNA synthesis by DNA polymerase kappa, the product of the human DINB1 gene. *J Biol Chem 275*: 39678–39684.
Roerink SF, Koole W, Stapel LC, Romeijn RJ, Tijsterman M. 2012. A Broad Requirement for TLS Polymerases η and κ, and Interacting Sumoylation and Nuclear Pore Proteins, in Lesion Bypass during C. elegans Embryogenesis. *PLoS Genet 8*: e1002800.
Shima N, Munroe RJ, Schimenti JC. 2004. The mouse genomic instability mutation chaos1 is an allele of Polq that exhibits genetic interaction with Atm. *Mol Cell Biol 24*: 10381–10389.
Tijsterman M, Pothof J, Plasterk RHA. 2002. Frequent germline mutations and somatic repeat instability in DNA mismatch-repair-deficient Caenorhabditis elegans. *Genetics 161*: 651–660.
Ye K, Schulz MH, Long Q, Apweiler R, Ning Z. 2009. Pindel: a pattern growth approach to detect break points of large deletions and medium sized insertions from paired-end short reads. *Bioinformatics 25*: 2865–2871.
Yousefzadeh MJ, Wood RD. 2012. DNA polymerase POLQ and cellular defense against DNA damage. *DNA Repair*.
Zhang Y, Wu X, Yuan F, Xie Z, Wang Z. 2001. Highly frequent frameshift DNA synthesis by human DNA polymerase mu. *Mol Cell Biol 21*: 7995–8006.